Journal of Neurochemistry

JOURNAL OF NEUROCHEMISTRY | 2014 | 128 | 280–293 doi: 10.1111/jnc.12505

ORIGINAL ARTICLE

Identification of two novel *Shank3* transcripts in the developing mouse neocortex

Chikako Waga,*,† Hirotsugu Asano,* Tomomi Sanagi,* Eri Suzuki,* Yasuko Nakamura,* Akiko Tsuchiya,* Masayuki Itoh,† Yu-ichi Goto,† Shinichi Kohsaka* and Shigeo Uchino*,‡

*Department of Neurochemistry, National Institute of Neuroscience, Kodaira, Tokyo, Japan

†Department of Mental Retardation and Birth Defect Research, National Institute of Neuroscience, Kodaira, Tokyo, Japan

‡Department of Biosciences, School of Science and Engineering, Teikyo University, Utsunomiya, Tochigi, Japan

Abstract

SHANK3 is a synaptic scaffolding protein enriched in the post-synaptic density of excitatory synapses. Since several SHANK*3* mutations have been identified in a particular phenotypic group of patients with autism spectrum disorder (ASD), SHANK3 is strongly suspected of being involved in the pathogenesis and neuropathology of ASD. Several SHANK3 isoforms are known to be produced in the developing brain, but they have not been fully investigated. Here, we identified two different amino-terminus truncated *Shank3* transcripts. One transcript, designated as *Shank3c-3*, produces an isoform that contains the entire carboxyl-terminus, but the other transcript, designated as *Shank3c-4*, produces a carboxyl-terminus truncated isoform. During development, expression of the novel *Shank3* transcripts increased after birth, transiently decreased at P14 and then gradually increased again thereafter. We also determined that methyl CpG-binding protein 2 (MeCP2) is involved in regulating expression of the novel *Shank3* transcripts. MeCP2 is a transcriptional regulator that has been identified as the causative molecule of Rett syndrome, a neurodevelopmental disorder that includes autistic behavior. We demonstrated a difference between the expression of the novel *Shank3* transcripts in wild-type mice and *Mecp2*-deficient mice. These findings suggest that the SHANK3 isoforms may be implicated in the synaptic abnormality in Rett syndrome.

Keywords: autism spectrum disorder, DNA methylation, MeCP2, SHANK3.

J. Neurochem. (2014) **128**, 280–293.

The *SHANK3/proline-rich synapse-associated protein 2 (PROSAP2)* gene consists of 22 exons and encodes a multidomain protein that contains ankyrin repeats (ANK) in an amino-terminal region, an Src homology 3 domain, a post-synaptic density 95/discs large/zone occludens-1 domain, a proline-rich region, a homer-binding region, a cortactin-binding region and a sterile alpha motif (SAM) (Naisbitt *et al.* 1999). SHANK3 is abundantly expressed in the heart and moderately expressed in the brain and spleen, and its tissue-specific expression is epigenetically regulated by DNA methylation (Lim *et al.* 1999; Beri *et al.* 2007). In the brain, SHANK3 is mainly expressed in neurons, especially in their synapses, and acts as a scaffolding protein in its interactions with various synaptic molecules, including with the NMDA receptor via the post-synaptic density-95 (PSD-95)/guanylate kinase-associated protein complex, with the metabotropic glutamate receptor via homer, and with the GluR1 alpha-amino-3-hydroxy-5-methylisoxazole-4-propionate receptor (Lim *et al.* 1999; Naisbitt *et al.* 1999; Sheng and Kim 2000; Boeckers *et al.* 2004; Uchino *et al.* 2006).

Received May 14, 2013; revised manuscript received October 2, 2013; accepted October 18, 2013.

Address correspondence and reprint requests to Shigeo Uchino, Department of Biosciences, School of Science and Engineering, Teikyo University, 1-1 Toyosatodai, Utsunomiya, Tochigi 320-8551, Japan. E-mail: uchino@nasu.bio.teikyo-u.ac.jp

Abbreviations used: AMPA, alpha-amino-3-hydroxy-5-methylisoxazole-4-propionate; ASD, autism spectrum disorder; MeCP2, methyl CpG-binding protein 2; SH3, Src homology 3; PDZ, post-synaptic density 95/discs large/zone occludens-1; SAM, sterile alpha motif.

Haploinsufficiency of the *SHANK3* gene causes a developmental disorder, 22q13.3 deletion syndrome, also known as Phelan-McDermid syndrome, which is characterized by severe expressive language and speech delay, hypotonia, global developmental delay, and autistic behavior (Bonaglia *et al.* 2001). Since numerous abnormalities in the *SHANK3* gene have been identified in a particular phenotypic group of patients with autism spectrum disorder (ASD), SHANK3 is strongly suspected of being involved in the pathogenesis and neuropathology of ASD (Durand *et al.* 2007; Moessner *et al.* 2007; Gauthier *et al.* 2009; Waga *et al.* 2011).

Several lines of *Shank3*-mutant mice have been generated and used to investigate the contribution of SHANK3 to the neuropathology of ASD (Bozdagi *et al.* 2010; Peça *et al.* 2011; Wang *et al.* 2011; Schmeisser *et al.* 2012; Yang *et al.* 2012; Jiang and Ehlers 2013). Mice that lack the full length of SHANK3 have been found to exhibit synaptic dysfunction and abnormal synaptic morphology and to display ASD-relevant phenotypes, including abnormal social behaviors, abnormal communication patterns, repetitive behaviors, and deficits in learning and memory, but several different SHANK3 isoforms were still expressed in the mutant mice. Peça and coworkers recently generated two *Shank3*-deficient mouse strains: a *Shank3A* mutant strain (*Shank3A*$^{-/-}$) lacking exons 4–7 and a *Shank3B* mutant strain (*Shank3B*$^{-/-}$) lacking exons 13–16 (Peça *et al.* 2011). The full length of SHANK3 (SHANK3α) is disrupted in *Shank3A*$^{-/-}$ mice but other isoforms are unaffected, whereas an amino-terminus truncated SHANK3 isoform lacking ANK (SHANK3β) as well as SHANK3α is absent in *Shank3B*$^{-/-}$ mice. Interestingly, a three-chamber social test demonstrated that the *Shank3B*$^{-/-}$ mice exhibited abnormal social interaction and discrimination of social novelty, whereas the *Shank3A*$^{-/-}$ mice, in which only SHANK3α is absent, displayed normal initiation of social interaction, but impaired recognition of social novelty. The *Shank3B*$^{-/-}$ mice displayed an anxiety-like behavior and excessive, self-injurious grooming, whereas the *Shank3A*$^{-/-}$ mice did not display any anxiety-like behavior and lesions. These findings suggest that dysfunction of the SHANK3 isoform is probably involved in the phenotypic heterogeneity in ASD.

Several SHANK3 isoforms are known to be produced in the mouse brain by combinations of multiple intragenic promoters and alternative splicing processes (Wang *et al.* 2011; Jiang and Ehlers 2013). The *SHANK3* gene contains five CpG islands (CpG-P and CpG-2 - CpG-5), and the positions of five CpG islands are well conserved in mammalian (Ching *et al.* 2005; Beri *et al.* 2007). Maunakea *et al.* recently demonstrated that some intragenic promoters are regulated by DNA methylation in CpG islands (Maunakea *et al.* 2010). However, the methylation status of the CpG islands in the *SHANK3* gene in the developing brain has not been fully investigated. In this study, we demonstrated differences between the methylation status of the five CpG islands in the developing mouse brain and identified novel SHANK3 transcripts whose transcriptional start sites are located in intron 10 in the vicinity of CpG island-2.

Materials and methods

Sequence of mouse *Shank3* gene

The genome sequence of the *Shank3* gene is available at the NCBI database (NC_000081.6), and the cDNA sequence is available at the GenBank database (AB231013).

Animals

The animals used in this study were Crl:CD-1 (ICR) mice (CLEA Japan, Tokyo, Japan), heterozygous *Mecp2*-deficient female mice (B6.129P2 (C)-*Mecp2* $^{tm1.1\ Bird/J}$; Jackson Laboratory, Maine, USA) (Guy *et al.* 2001) and C57BL/6JJcl male mice (CLEA Japan), which were used for mating with *Mecp2*-deficient female mice. All experimental procedures were approved by The Animal Care and Use Committee of the National Institute of Neuroscience.

Analysis of the methylation status of the CpG islands

Genomic DNA was extracted from mouse neocortical tissue (gray matter) at embryonic day 17 (E17), post-natal day 1 (P1), P7, P14, P21, P28, and 12 weeks after birth (12W) using the Wizard Genomic DNA Purification Kit (Promega, Madison, WI, USA). Three mice were used at each developmental stage. Methylation status was determined by the *Hpa*II-*Mcr*BC PCR method using two restriction enzymes having complementary methylation sensitivity, *Hpa*II and *Mcr*BC, as described in a previous study (Yamada *et al.* 2004). PCR was performed by using PrimeSTAR DNA polymerase (Takara, Shiga, Japan) and a thermal cycler (GeneAmp PCR System 9700; Life Technologies, Grand Island, NY, USA). The primer sequences, annealing temperatures, cycles, and sizes of the PCR products are shown in Table S1. The following primer pairs were used: CpGP-F/CpGP-R for CpG island-P, In10-F/CpG2-R for CpG island-2, CpG3-F/CpG3-R for CpG island-3, CpG4-F/CpG4-R for CpG island-4, CpG5-F/CpG5-R for CpG island-5, and 5UTR-F/5UTR-R as a control. The thermocycling conditions were: 60 s at 98°C, 30 s at the annealing temperature, 60 s at 72°C for 33–45 cycles. The PCR products were electrophoretically separated on an agarose gel and stained with ethidium bromide. The gel images were fed into an image analyzer (LAS-3000 mini; FUJIFILM, Tokyo, Japan) and quantitatively analyzed with ImageJ software (National Institutes of Health, Bethesda, MD, USA). The data were obtained from three independent PCR experiments.

Total RNA preparation, cDNA synthesis, and real-time PCR

Total RNA was extracted from mouse neocortical tissue (gray matter) with acid guanidinium thiocyanate–phenol–chloroform at E17, P1, P7, P14, P21, P28, and 12W (Chomczynski and Sacchi 1987), and cDNA was produced by using the Advantage RT for PCR kit (Clontech, Palo Alto, CA, USA) according to the manufacturer's instructions. Three mice were used at each developmental stage.

PCR for analysis of expression of the novel *Shank3* transcripts was performed using PrimeSTAR DNA polymerase with GC buffer (Takara) and a thermal cycler (GeneAmp PCR System 9700). The thermocycling conditions were: 60 s at 98°C, 30 s at 60°C, 60 s at 72°C for 40 cycles for brain tissue and 45 cycles for Neuro2A cells. The primers used were In10-F and Ex14-R, and their sequences are listed in Table S2.

Real-time PCR was performed by using the SYBR green labeling system (Power SYBR Green PCR Master Mix; Life Technologies) and the ABI Prism 7700 Sequence Detection System (Life Technologies). The primer sequences and sizes of the PCR products are shown in Table S2. Amplifications were carried out in a 384-well optical plate, and the thermocycling conditions were: 5 s at 95°C, 10 s at 60°C, and 30 s at 72°C for 45 cycles. A quantitative analysis was performed by the delta-delta Ct method with glyceraldehyde-3-phosphate dehydrogenase used as an internal control (Ermolinsky *et al.* 2008). The data were obtained from four independent PCR experiments.

5′-Rapid Amplification of cDNA Ends (5′-RACE)

Total RNA was prepared from the neocortical tissue (gray matter) of P14 mice, and 5′-RACE was performed by using the GeneRacer kit (Life Technologies) according to the manufacturer's instructions. PCR was performed by using AmpliTaq Gold 360 Master Mix (Life Technologies) and a thermal cycler (GeneAmp PCR System 9700). The initial thermocycling conditions were as follows: 30 s at 98°C and 60 s at 72°C for 5 cycles, 30 s at 98°C and 60 s at 70°C for 5 cycles, and then 30 s at 98°C, 30 s at 65°C, 60 s at 72°C for 30 cycles, and the primers used were GeneRacer 5′-primer (5′-CGACTGGAGCACGAGGACACTGA-3′) and Ex14-R2 primer (5′-GGATAGCCACCTTATCATCGATGACATAATCG-3′). The second thermocycling conditions were: 30 s at 98°C, 30 s at 65°C, 60 s at 72°C for 30 cycles, and the primers used were the GeneRacer 5′-Nested primer (5′-GGACACTGACATGGACT GAAGGAGTA-3′) and Ex14-R2 primer. The PCR product was subcloned into pGEM-T Easy vector (Promega) by the TA cloning method, and the DNA sequence was determined by using an ABI3100-*Avant* genetic analyzer (Life Technologies).

Identification of *Shank3* transcripts

The full length of the *Shank3* transcript expressed from the intron 10 region was cloned by the RT-PCR method. The cDNA produced from neocortical total RNA at P14 was used as a template DNA. PCR was performed using KOD-plus- (TOYOBO, Tokyo Japan) and a thermal cycler (GeneAmp PCR System 9700). The thermocycling conditions were: 10 s at 98°C and 8 min at 68°C for 5 cycles, and then 10 s at 98°C, 30 s at 62°C, 8 min at 68°C for 30 cycles, and the primers used were In10-F and 3UTR-R (5′-AGGG CCCCCCACCCCACAGGTCATT-3′). The PCR products were subcloned into pGEM-T Easy vector (Promega) by the TA cloning method, and at least two different *Shank3* constructs were obtained: pGEM-Shank3c-3, which contained part of the sequence coded by intron 10 and a completely spliced form from exon 11 to exon 22, and pGEM-Shank3c-4, which lacked the sequences coded by exon 21. The DNA sequences were determined with an ABI3100-*Avant* genetic analyzer.

Plasmid construction

The construction of the plasmids used in this study is described in detail in the experimental procedure and Figure S1 and Figure S2 in the supplemental information.

Cell culture and DNA transfection

Neuro2A cells and HEK293 cells were grown at 37°C in Dulbecco's modified Eagle's medium (Life Technologies) containing 10% heat-inactivated fetal bovine serum under a humidified 5% CO_2 atmosphere. Neuro2A cells were plated at a density of 1.0–3.0 $\times$ 10^4 cells/cm^2 and maintained for 2 days in medium containing a 1 μM or 5 μM concentration of 5-Aza-2′-deoxycytidine (5-AdC; Wako, Osaka, Japan). For the luciferase assays, HEK293 cells were plated in each well of 12-well culture dishes at a density of 5.0 $\times$ 10^4 cells/well, maintained for 2 days, and then transfected with a plasmid DNA by using TransIT-LT1 (Mirus Bio, Madison, WI, USA) according to the manufacturer's instructions. After 2 days, the cells were harvested and used for the luciferase assay. For immunoblot analysis, HEK293 cells were plated at a density of 1.0 $\times$ 10^4 cells/cm^2, maintained for 2 days, and then transfected with a plasmid DNA by using Lipofectamine Plus (Life Technologies) according to the manufacturer's instructions. After 2 days, the cells were harvested and used for the immunoblot analysis.

Embryonic day 15.5 ICR mouse neocortical primary neurons were prepared as described previously (Hirasawa *et al.* 2003). Briefly, cerebral cortices were dissected, minced and dissociated with papain. The dissociated cells were plated onto 0.1% polyethyleneimine-coated plates at a density of 1.5–3.0 $\times$ 10^4 cells/cm^2 for immunocytochemistry and at a density of 5.0 $\times$ 10^4 cells/cm^2 for luciferase assays, and maintained in Neurobasal (NB) medium (Life Technologies) containing 2% B-27 supplement (Life Technologies) and 0.5 mM glutamine (NB-s-medium) at 37°C under a humidified 10% CO_2 atmosphere for the indicated periods. For the transient expression studies, cells were transfected with a plasmid DNA by using Lipofectamine 2000 (LF2000; Life Technologies) according to the manufacturer's instructions, with slight modifications. Plasmid DNA that had been diluted with NB medium and LF2000 Reagent that had been diluted with NB medium were combined and incubated for 15–20 min at 20–25°C. The DNA-LF2000 Reagent complex was added to the cells, and they were maintained at 37°C in a 10% CO_2 incubator for 1–2 h. After washing with fresh NB medium the cells were maintained in conditioned medium that consisted of equal volumes of fresh NB medium and spent medium harvested from cultured cells. Half of the medium was replaced with fresh NB-s-medium every 3–4 days.

Luciferase assay

Luciferases assays were performed by using the Dual-Luciferase Reporter Assay System (Promega) according to the manufacturer's instructions, and reporter activity was measured with a Centro LB960 plate reader (Berthold Technologies, Bad Wildbad, Germany). The firefly luciferase value of each sample was divided by the renilla luciferase value to average the independent transfection. Each plasmid was transfected into cells cultured in three separate wells, and three independent transfections were performed.

Immunocytochemistry

Cells were fixed with 2% paraformaldehyde for 10 min at 20–25°C. After three washes with phosphate-buffered saline (PBS) at 5-min intervals, the cells were permeabilized and blocked in PBS containing 3% normal goat serum and 0.1% Triton X-100 for 15 min, and then incubated for 1 h at 20–25°C with the following primary antibodies in PBS containing 3% bovine serum albumin : rabbit polyclonal anti-enhanced green fluorescent protein (EGFP) antibody (1 : 500, Life Technologies), mouse monoclonal anti-MAP-2 antibody (1 : 500, Sigma, St Louis, MO, USA), rabbit polyclonal anti-Shank3 antibody (1 : 1000) (Uchino *et al.* 2006), or mouse monoclonal anti-myc antibody (clone 9E10) (1 : 300, Thermo Scientific, Rockford, IL, USA). After washing three times with PBS at 5-min intervals, the cells were incubated for 1 h at 20–25°C with the secondary antibodies in PBS containing 3% bovine serum albumin: Alexa Fluor 488 goat anti-rabbit IgG (H+L) (1 : 1000, Life Technologies), Alexa Fluor 488 goat anti-mouse IgG (H+L) (1 : 1000, Life Technologies), Alexa Fluor 594 goat anti-rabbit IgG (H+L) (1 : 1000, Life Technologies), or Alexa Fluor 594 goat anti-mouse IgG (H+L) (1 : 1000, Life Technologies). After washing three times with PBS at 5-min intervals, the cells were mounted on a glass slide with Fluoro-mount-G (Southern Biotech, Birmingham, AL, USA). Fluorescence images were obtained with a fluorescence microscope (AX70; Olympus, Tokyo, Japan) or a confocal laser microscope (FV1000; Olympus).

Preparation of protein samples and immunoblot analysis

HEK293 cells or neocortex tissue were homogenized and sonicated in lysis buffer (10 mM Tris-HCl (pH 7.4), 150 mM NaCl, 1 mM EDTA, 1% Triton X-100, 0.1% sodium dodecyl sulfate and a protease inhibitor cocktail (Roche, Penzberg, Germany). After removing the nuclei and debris by centrifugation (2000 x *g* for 10 min at 4°C), the protein concentration of the supernatant was determined using BCA Protein Assay Kit (Pierce, Rockford, IL, USA), and the supernatant was stored at −80°C until used.

The protein samples were separated by electrophoresis through an sodium dodecyl sulfate polyacrylamide gel: a 5% gel for neocortical samples and a 5–20% gradient gel (Dream Realization & Communication (DRC), Tokyo, Japan) for HEK293 cells, and then electrophoretically transferred to nitrocellulose membranes (Schleicher & Schuell, Dassel, Germany). The membranes were blocked overnight with 3% skim milk in Tris-buffered saline containing 0.1% Tween20 (TBS-T) at 4°C, then incubated at 20–25°C for 3 h in 3% skim milk in TBS-T containing rabbit polyclonal anti-Shank3 antibody (1 : 3000) (Uchino *et al.* 2006), mouse monoclonal anti-myc antibody (clone 9E10) (1 : 1500), or mouse monoclonal anti-β actin antibody (1 : 1500; Sigma). After three washes in TBS-T, the membranes were incubated at 20–25°C for 1 h with horseradish peroxidase-conjugated anti-rabbit IgG secondary antibody (1 : 1500; Sigma) or horseradish peroxidase-conjugated anti-mouse IgG secondary antibody (1 : 1500; GE Healthcare, Buckinghamshire, UK), and washed three times with TBS-T. Immunoreactive bands were visualized with a chemiluminescence detection system (ECL; GE Healthcare) and the images were fed into an image analyzer (LAS-3000 mini).

Chromatin immunoprecipitation (ChIP)

Fresh mouse neocortical tissue (gray matter, 100–150 mg) was dissected out, chopped into small pieces, and homogenized. ChIP was performed by using the ChIP assay kit (Millipore, Temecula, CA, USA) and rabbit polyclonal anti-Mecp2 antibody (Millipore) according to their manufacturers' instructions. PCR was performed by using GoTaq DNA polymerase (Promega) and a thermal cycler (GeneAmp PCR System 9700). The primer sequences, annealing temperatures, and sizes of the PCR products are shown in Table S1. The primer pairs used were: In10-F/CpG2-R for CpG island-2, CpG3-F/CpG3-R for CpG island-3, CpG4-F/CpG4-R for CpG island-4, and CpG5-F/CpG5-R and CpG5-F2/CpG5-R for CpG island-5. The thermocycling conditions were as follows: 30 s at 98°C, 30 s at annealing temperatures, 60 s at 72°C for 45 cycles. The PCR with the In10-F and CpG2-R primer pair was performed under 5% dimethyl sulfoxide.

Statistical analysis

All values were expressed as the mean ± SEM of *n* independent observations. Multiple groups were compared by one-way analysis of variance (ANOVA), which was followed by Dunnett's test when two groups were compared. Differences were considered significant when the *p*-value was < 0.05.

Results

Methylation analysis of the CpG islands in the mouse *Shank3* gene

To investigate the methylation status of the five CpG islands (CpG-P and CpG-2 - CpG-5 shown in Fig. 1a) in the developing mouse brain, genomic DNA was extracted from mouse neocortical tissue at E17, P1, P7, P14, P21, P28, and 12 weeks after birth (12W), and the methylation status of the CpG islands was assessed by the *Hpa*II-*Mcr*BC PCR method (Yamada *et al.* 2004). *Hpa*II digests unmethylated alleles at CCGG sites, and *Mcr*BC digests methylated alleles at $Pu^{m}C(N_{40–2000})Pu^{m}C$, When a sequence is fully methylated, *Hpa*II fails to digest the target site, whereas *Mcr*BC digests it completely. Therefore, a PCR product of a target region is detected only from the *Hpa*II-digested template. Since PCR products at CpG island-P were detected only from the *Mcr*BC-digested template (lane U in Fig. 1b) and PCR products at CpG island-3 were detected only from the *Hpa*II-digested template (lane M in Fig. 1b), the results showed that CpG island-P was completely unmethylated and CpG island-3 was fully methylated at every stage of development investigated, whereas the methylation rate of CpG island-2, -4, and -5 were low in the embryonic stage, but significantly increased after birth. Interestingly, the methylation rate of CpG island-2 increased until P14 and gradually decreased thereafter (Fig. 1b and c).

A novel *Shank3* transcript in intron 10

Since Beri and coworkers reported finding dramatic differences in the methylation status of CpG island-2 in various

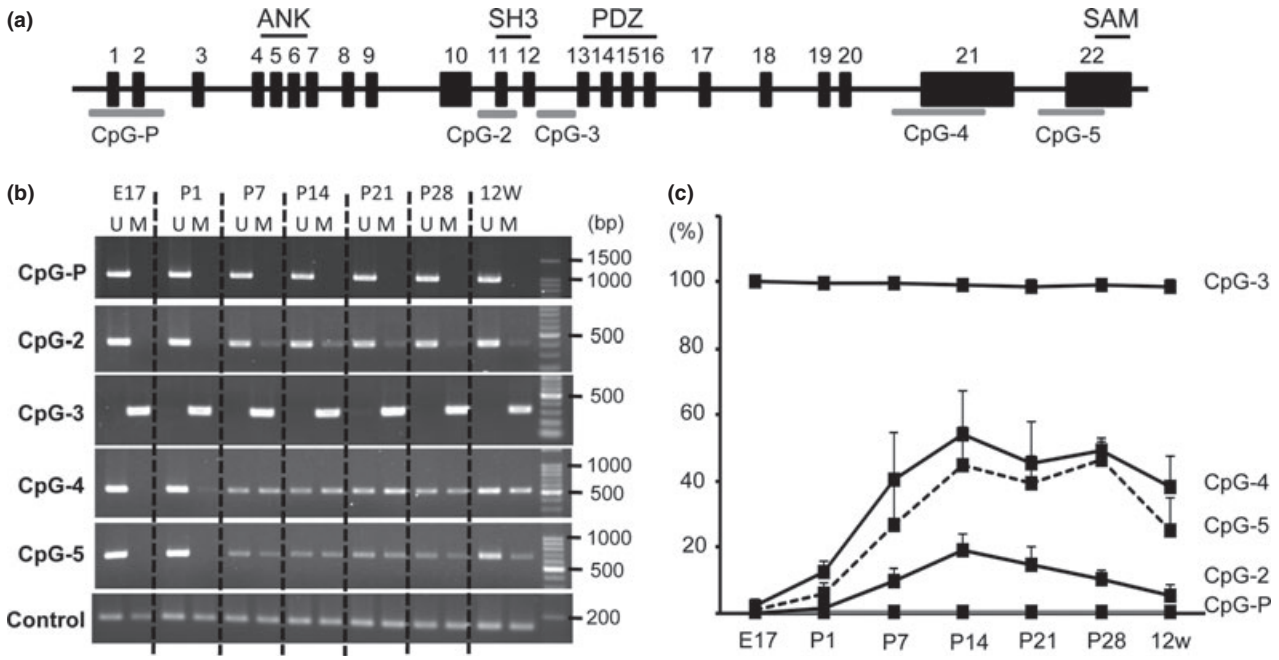

Fig. 1 Methylation status of the intragenic CpG-islands of the *Shank3* gene in the developing mouse neocortex. (a) Schematic structure of the mouse *Shank3* gene. Exons (1–22) are represented by a black box, and the CpG islands identified by using a Methyl Primer Express software (Life Technologies) are represented by a gray line. (b) Representative agarose gel electrophoresis images showing a *Hpa*II-*Mcr*BC PCR assay of the five CpG islands in the *Shank3* gene. A *Hpa*II-digested template (M) and an *Mcr*BC-digested template (U) were used. Size markers (100 bp ladder) are shown at the right. (c) Quantitative analysis of methylation status determined by a *Hpa*II-*Mcr*BC PCR assay. $n = 3$.

tissues and cell lines (Beri *et al.* 2007), we focused on CpG island-2. Because genome sequence analysis revealed high homology (94%) between an approximately 380 bp length of DNA containing CpG island-2 located upstream of exon 11 in the human gene and the mouse gene (Fig. 2a), we hypothesized expression of a novel transcript in this intragenic region. To test our hypothesis we performed RT-PCR using a forward primer within intron 10 (In10-F) and a reverse primer within exon 14 (Ex14-R), and an approximately 450 bp PCR product was detected as a result. Sequence analysis revealed that the PCR product contained part of intron 10 and a completely spliced form from exon 11 to exon 14 of the *Shank3* gene (Fig. 2b). Expression of this transcript was weak at E17 but increased after birth. Interestingly, its expression transiently decreased at P14, when the methylation rate in CpG island-2 was the highest, but increased thereafter (Fig 2c). We quantified its expression level in the developing mouse brain by a real-time PCR (Fig. 2d). To determine whether expression of the novel transcript is regulated by DNA methylation, we examined its expression in Neuro2A cells cultured for 2 days in the presence or absence of the DNA methylation inhibitor 5-AdC. As shown in Figure 2e, exposure to 5-AdC resulted in an increase in expression of the novel transcript in comparison with the control Neuro2A cells, suggesting that expression of the novel transcript is regulated by DNA methylation.

Identification of the entire sequence of the novel *Shank3* transcript in intron 10

To identify the transcriptional initiation site of the novel *Shank3* transcript, we performed a 5′-RACE-PCR, and as shown in Fig. 3, the results revealed a transcriptional initiation site (−265) in intron 10. Sequence analysis revealed two putative sites of the translational start codon (ATG): one in intron 10 and the other in exon 12 (Fig. 3a). Since Maunakea and coworkers recently found promoter activity that is regulated by intragenic DNA methylation in the upstream of CpG island-2 in intron 10 (ECR22-promoter shown in Fig. 2a), and showed that the ECR22-promoter regulates expression of the 22t *Shank3* transcript (shown in Fig. 3b) (Maunakea *et al.* 2010), we next attempted to confirm the promoter activity of the intron 10 by using a luciferase assay system. We constructed a reporter vector carrying a 297 bp or a 610 bp length of the intragenic gene containing the ECR22-promoter region (pGL3-ECR22-pro and pGL3-In10-pro, respectively, shown in Fig. 4a), and transfected it into HEK293 cells. Measurement of the luciferase activity 2 days later confirmed the presence of promoter activity in the ECR22-promoter regions

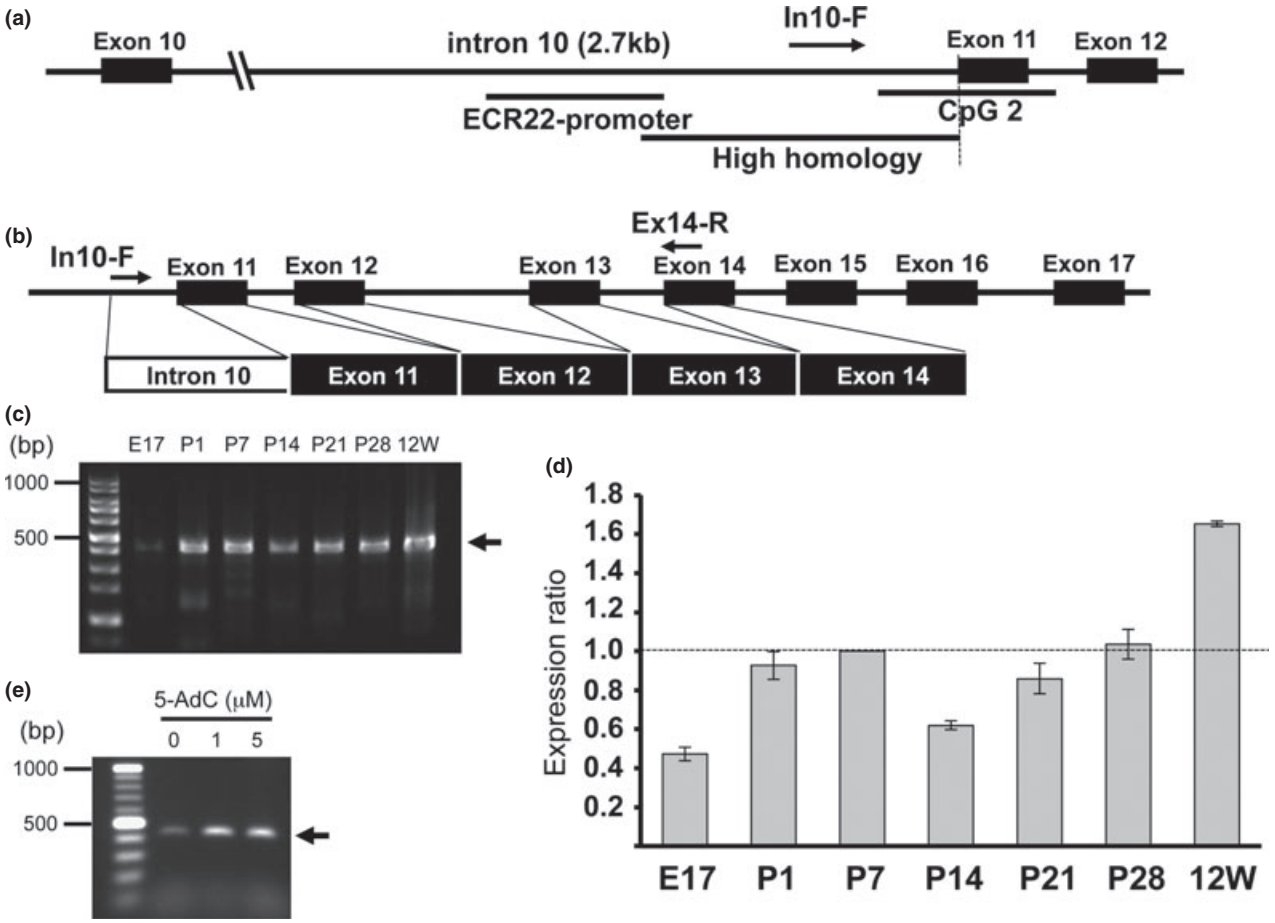

Fig. 2 Gene structure and expression profile of the novel *Shank3* transcript in intron 10. (a) Schematic structure of the mouse *Shank3* gene. Exons (10–12) are represented by a black box, and CpG island-2, a higher homology region between humans and the mouse, and the ECR22-promoter region (Maunakea *et al.* 2010) are each represented by a black line. (b) Schematic diagram of the novel *Shank3* transcript amplified by the In10-F and Ex14-R primer pair. (c) Representative agarose gel electrophoresis image showing expression of the novel *Shank3* transcript in the developing mouse neocortex after the transcript was amplified by an RT-PCR method. The arrow points to the PCR product (441 bp) amplified by the In10-F and Ex14-R primer pair. Size markers (100 bp ladder) are shown at the left. (d) Quantitative analysis of expression of the novel *Shank3* transcript by a real-time PCR using the delta-delta Ct method with glyceraldehyde-3-phosphate dehydrogenase as an internal control. The ratios were calculated by dividing the value at each stage by the value at P7. $n = 4$. (e) Representative agarose gel electrophoresis image showing expression of the novel *Shank3* transcript in Neuro2A cells in the presence of 5-AdC (1 μM, 5 μM) and in the absence of 5-AdC (0 μM). Size markers (100 bp ladder) are shown at the left.

(3.72 ± 0.12 fold), the same as found in a previous study (Maunakea *et al.* 2010), but no promoter activity was detected in the 610 bp length of the intragenic region (0.87 ± 0.06 fold) (Fig. 4b). Since sequence analysis revealed the presence of three ATG sequences within the 610 bp length of the intron region, when the ATG sequences function as a translational start codon luciferase may not be produced because of a frameshift. We then constructed two different reporter vectors, one lacking the adenine nucleotide at two positions, −293 and −186 (pGL3-In10-pro-ΔATG-2), and the other lacking the adenine nucleotide at three positions, −293, −186, and −77 (pGL3-In10-pro-ΔATG-all), in order to disrupt the ATG codon (Fig. 4a), and after transfecting each of the constructs into HEK293 cells, we measured their luciferase activity. Significant luciferase activity was observed in the cell lysate prepared from the HEK293 cells transfected with pGL3-In10-pro-ΔATG-all (2.23 ± 0.21 fold), but no luciferase activity was detected in the cell lysate prepared from the HEK293 cells transfected with pGL3-In10-pro-ΔATG-2 (0.97 ± 0.04 fold) (Fig. 4b), suggesting that the ATG sequence at position −77 functions as the translational start codon. We also confirmed the presence of luciferase activity in neocortical primary neurons transfected with pGL3-ECR22-pro (3.41 ± 0.21 fold) and pGL3-In10-pro-ΔATG-all (9.42 ± 0.67 fold) (Fig. 4c). Next, we constructed an expression vector containing an EGFP gene ligated at the ATG site at position −77 (Fig. 4a, Figure S1) and

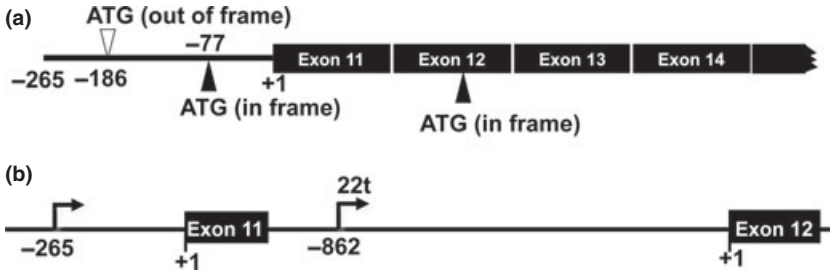

Fig. 3 Identification of the novel *Shank3* transcripts in intron 10. (a) The 5′-gene structure of the novel *Shank3* transcripts. The predicted translational start codon (ATG) is indicated by a closed arrowhead (in frame). (b) Schematic structure of the mouse *Shank3* gene. Exons 11 and 12 are represented by a black box and transcriptional initiation site of the novel *Shank3* transcript (at−265 in intron 10) and the transcriptional initiation site of 22t *Shank3* (at−862 in intron 11) (Maunakea *et al.* 2010) are each indicated by an arrow.

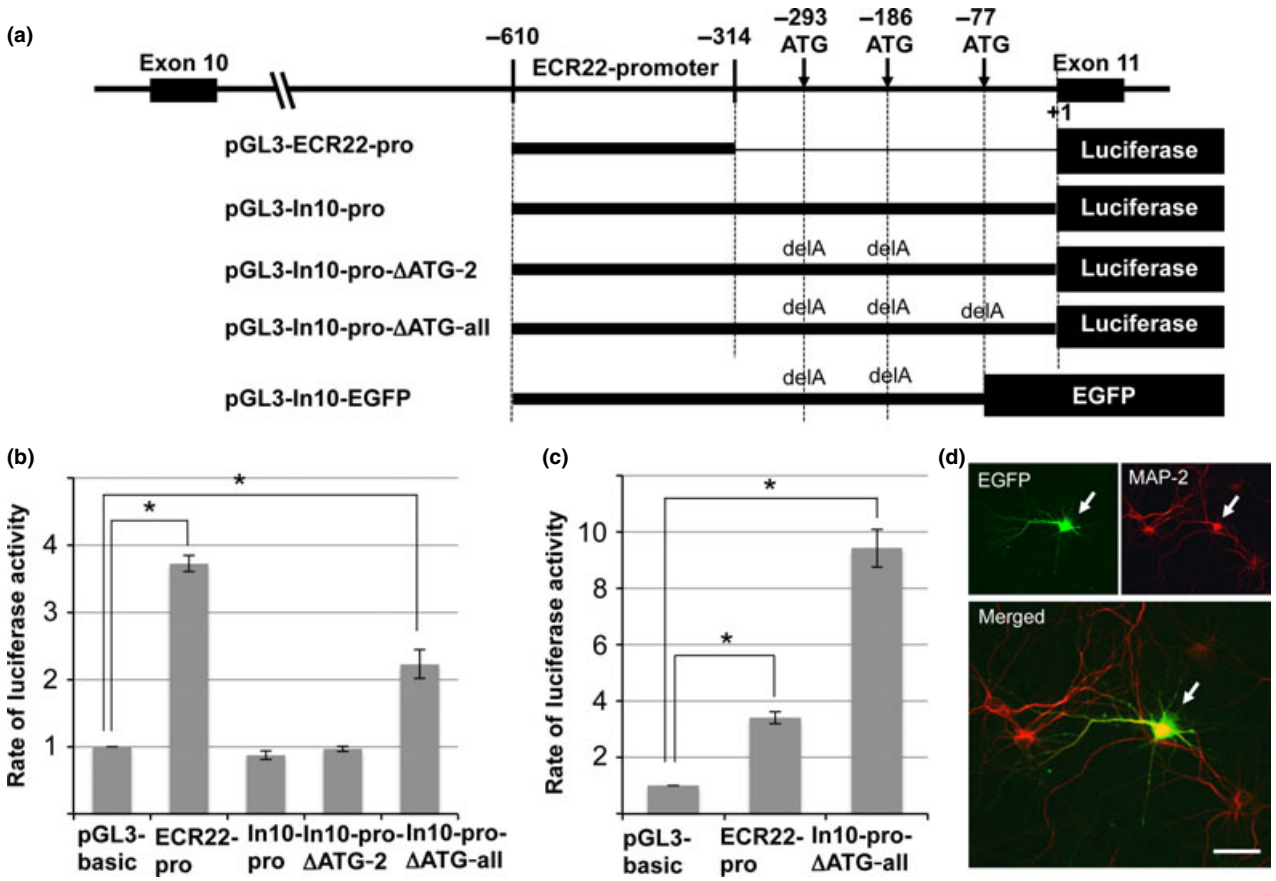

Fig. 4 Promoter activity of the DNA fragment within intron 10. (a) Schematic structure of the constructs used for the luciferase assay and enhanced green fluorescent protein (EGFP) expression. (b) Luciferase assay. HEK293 cells were transfected with the constructs, and 2 days later the cells were harvested and used for a luciferase assay. The ratios were calculated by dividing the value of each sample by the value of the control sample (pGL3-basic). *$p < 0.01$. (c) Luciferase assay. Neocortical primary neurons were cultured for 8 days and transfected with the constructs, and 2 days later the cells were harvested and used for the luciferase assay. The ratios were calculated by dividing the value of the each sample by the value of the control sample (pGL3-basic). *$p < 0.01$. (d) Representative image of immunostained neurons. Neocortical primary neurons were cultured for 8 days and transfected with pGL3-In10-EGFP, and 2 days later the cells were fixed and immunostained with anti-EGFP antibody (green) and anti-MAP-2 antibody (red). The arrow points to an EGFP- and MAP-2-positive cell. Scale bar is 20 μm.

transfected it into neocortical primary neurons that had been cultured for 8 days, and 2 days later we detected the EGFP fluorescent signal in neurons (Fig. 4d). These findings suggested that the ATG sequence at position −77 functions as a translational start codon in neurons.

Finally, we cloned the entire novel *Shank3* transcript by using the RT-PCR method and an In10-F primer and a reverse primer within the 3′-untranslated region (UTR) (3UTR-R) and detected a PCR product of about 5 kb. Sequence analysis confirmed that this PCR product completely matched the spliced *Shank3* transcript from exon 11 to exon 22 (Fig. 5). As shown in Figure 2c the expression profile of this transcript in the developing brain was similar to the expression profile of 441 bp of the PCR product (Fig. 5a). Notably, the level of expression of this transcript at P14 was lower than that at P7 and P21. We also detected other transcripts of different sizes (about 3 kb), especially at P7 and P14 (Fig. 5a), and sequence analysis identified one of the PCR products as the transcript that lacked the sequence coded by exon 21. Since the transcript caused a frameshift in ligation with exon 20 to exon 22, it may produce the carboxyl-terminus truncated isoform that lacked a homer-binding region, a cortactin-binding region and an SAM (Fig. 5b). These findings indicated the existence of two different *Shank3* transcripts whose transcriptional initiation site is located in intron 10.

In the recent review by Jiang and Ehlers, the *Shank3c* transcripts are expressed under the control of promoter 3 located in intron 10 (Jiang and Ehlers 2013), and Wang and coworkers have identified two *Shank3c* transcripts (*Shank3c-1* and *Shank3c-2*; GenBank HQ405757 and HQ405758) (Wang *et al.* 2011). We therefore designated the novel *Shank3* transcripts found in this study *Shank3c-3* (a completely spliced form from exon 11 to exon 22; GenBank AB841411) and *Shank3c-4* (deletion of exon 21; GenBank AB841412).

Expression profile of the novel SHANK3c isoforms in the developing mouse neocortex

We next investigated the expression of the novel SHANK3c isoforms in the developing mouse neocortex by an immunoblot analysis. First, we constructed three expression vectors that produce the myc-tagged SHANK3 isoforms, SHANK3a (full-length SHANK3), SHANK3c-3 and SHANK3c-4, transfected them into HEK293 cells, and determined the molecular size of the SHANK3 isoforms by immunoblot analysis with anti-myc antibody. As shown in Figure 6a, the SHANK3 isoforms had their expected molecular sizes: myc-SHANK3a consisted of 1730 amino acids (aa) plus 22 extra sequences aa that included myc-tag, myc-SHANK3c-3 of 1322 SHANK3c-3 aa plus 22 aa, and myc-SHANK3c-4 of 382 SHANK3c-4 aa plus 22 aa. Since the anti-Shank3 antibody we used recognizes the peptides coded within exon 21 (Uchino *et al.* 2006), myc-SHANK3c-4 was not detected by immunoblotting with anti-Shank3 antibody. Next, we identified the immunoblot bands that corresponded to the SHANK3a and SHANK3c-3 isoforms based on their molecular sizes (Fig. 6b) and examined the expression profile of the SHANK3 isoforms in the developing neocortex (Fig. 6c). The results of the immunoblot analysis suggested that SHANK3a expression increased during development but that expression of SHANK3c-3 transiently decreased at P21. However, since we have not yet developed a specific antibody for SHANK3c, further study will be necessary to draw any conclusions about the expression profiles of the SHANK3 isoforms.

Difference between the distribution of SHANK3c isoforms with and without the carboxyl terminus expressed in neocortical primary neurons

Since a cortactin-binding region and an SAM are essential for SHANK3 targeting to synapses and clustering (Boeckers

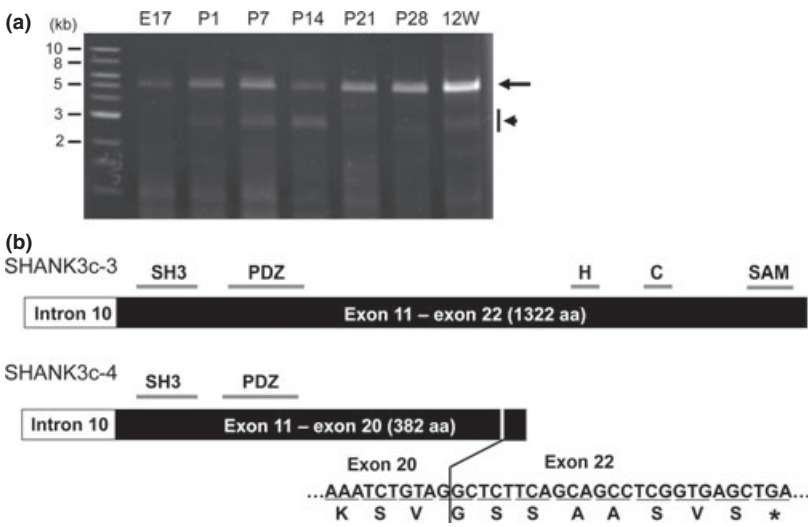

Fig. 5 SHANK3 isoforms expressed from intron 10. (a) Representative agarose gel electrophoresis image showing expression of *Shank3* transcripts in the developing mouse neocortex. The arrow points to the *Shank3* transcript that contains exon 11 - exon 22, and the arrowhead points to the several alternative splicing variants. Size markers (1 kb ladder) are shown at the left. (b) Schematic structure of SHANK3c-3, the novel SHANK3 isoform with all exons from exon 11 to exon 22, and SHANK3c-4, its alternative splicing variant, which lacks exon 21. H, homer-binding region; C, cortactin-binding region.

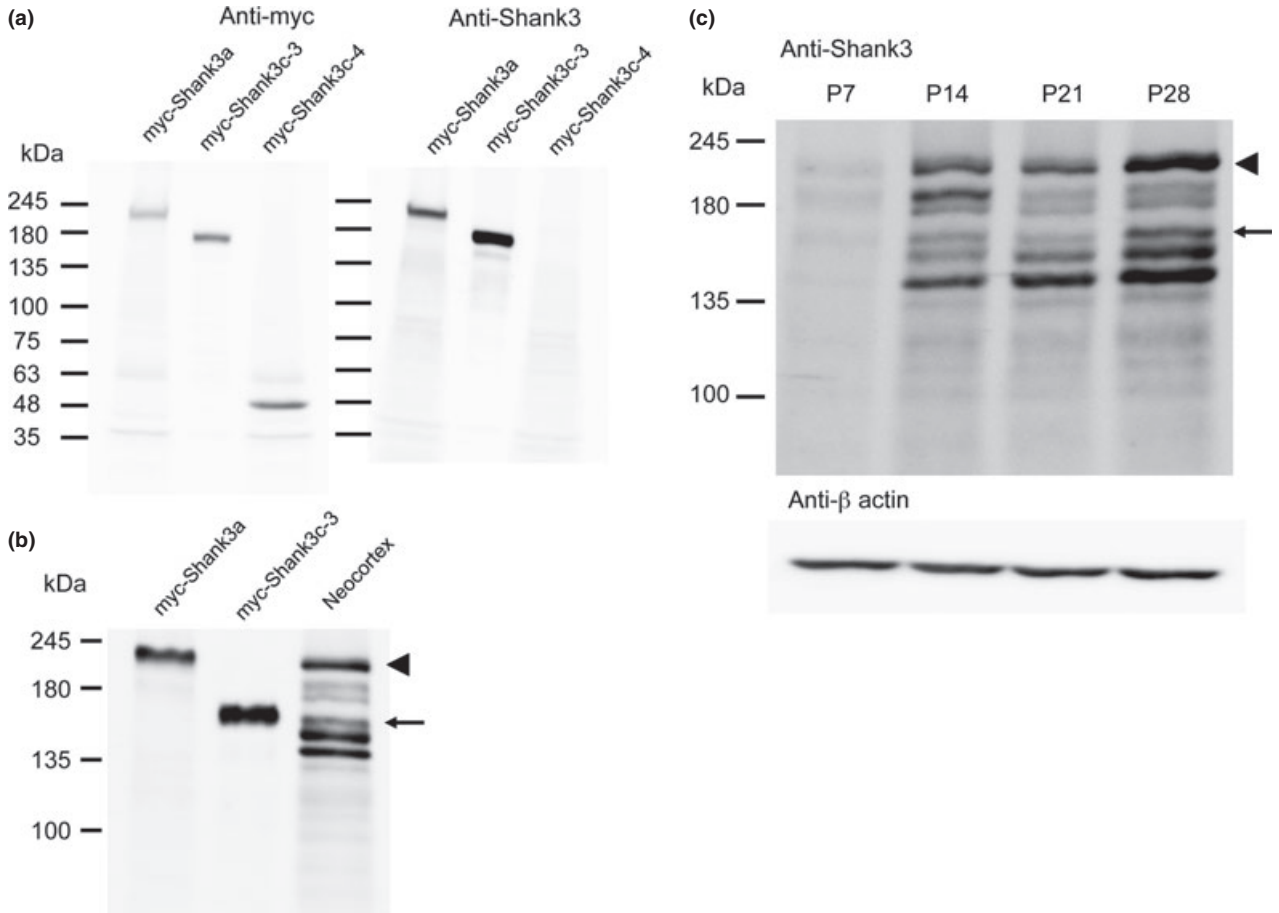

Fig. 6 Expression profile of SHANK3c isoforms in the developing mouse neocortex. (a) Immunoblot analysis with anti-myc antibody (left panel) and anti-Shank3 antibody (right panel). Molecular weight standards are shown on the left. (b) Immunoblot analysis with anti-Shank3 antibody. A neocortical sample prepared from a mouse at P28 (50 μg) was loaded. The arrow indicates SHANK3c-3 and the arrowhead indicates SHANK3a. (c) Immunoblot analysis with anti-Shank3 antibody (upper panel) and anti-β actin (lower panel). Neocortical samples (50 μg) were loaded. The arrow indicates SHANK3c-3, and the arrowhead indicates SHANK3a.

et al. 2005), we examined the distribution of the carboxyl-terminus truncated SHANK3c-4 isoform that lacked the sequence coded by exon 21. We constructed two expression vectors carrying myc-tagged Shank3c-3 and Shank3c-4, whose translational start codon (ATG) is at position -77 in intron 10, under the CAG promoter (Fig. 3a, 5b, S2), and co-transfected each construct into neocortical primary neurons cultured for 9 days with the pCAGGS-EGFP plasmid to visualize the transfected neurons. After 7 days of culture, we fixed the cultured neurons and immunostained them with anti-myc antibody and anti-Shank3 antibody or anti-EGFP antibody. There was a close match between the immunoreactive signals obtained with anti-Shank3 antibody and anti-myc antibody in the transfected neurons (Fig. 7a). Judging from the morphology of the EGFP-positive neurites, the punctate expression signals of myc-Shank3c-3 were predominantly detected in the dendrites and few signals were detected in the axons (Fig. 7b). In contrast, the expression signals of myc-Shank3c-4 were diffusely observed in both the dendrites and axons (Fig. 7b). These results indicated that there is a large difference in synaptic localization between the two SHANK3c isoforms.

MeCP2 binds the *Shank3* gene at the methylated CpG islands

To identify related molecules involved in expression of the novel *Shank3c* transcripts, we focused on MeCP2, which has been identified as the causative molecule of Rett syndrome and is thought to regulate gene transcription, mRNA splicing, and chromatin structure (Amir *et al.* 1999; Lam 2000; Hite *et al.* 2009). We investigated whether MeCP2 binds the methylated CpG islands of the *Shank3* gene by performing a ChIP assay. The results showed that at P1 MeCP2 bound CpG island-3 alone, but at P14 bound CpG island-2 and -4 in addition to CpG island-3 (Fig. 8). However, even though CpG island-5 was methylated the same as CpG island-4, no PCR product for CpG island-5 was detected even when two primer pairs were used (Fig. 8). No MeCP2 binding at CpG

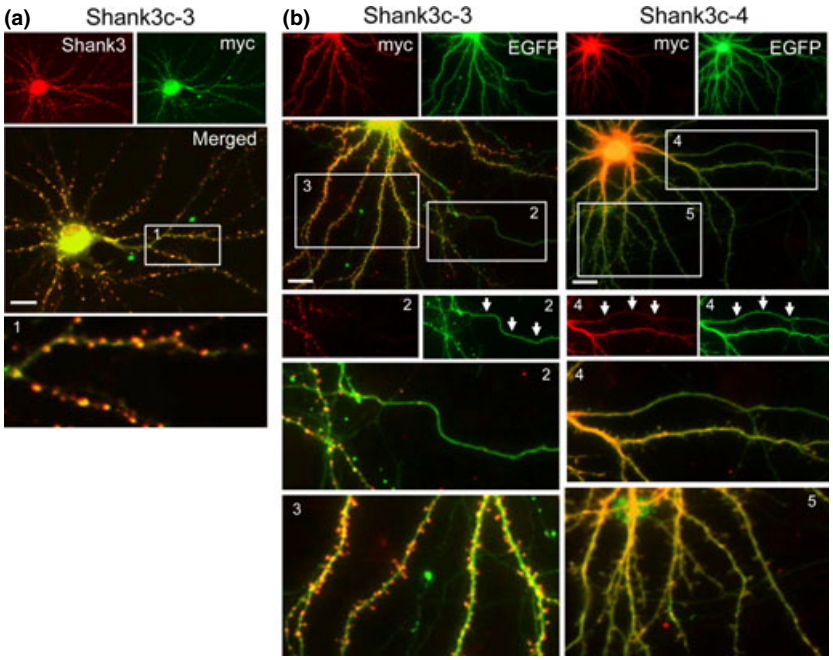

Fig. 7 Difference between the distribution of SHANK3c isoforms with and without the carboxyl terminus expressed in neocortical primary neurons. Representative image of immunostained neurons. Neocortical primary neurons prepared from E15.5 mice were cultured for 9 days and co-transfected with pCAGGS-enhanced green fluorescent protein (EGFP) and the expression vector, pCAGGS-myc-Shank3c-3 or pCAGGS-myc-Shank3c-4. After culture for an additional 7 days cells were fixed and double-stained with anti-Shank3 antibody (red) and anti-myc antibody (green) (a) and with anti-myc antibody (red) and anti-enhanced green fluorescent protein (EGFP) antibody (green) (b). Enlarged images of each of the numbered boxes are shown. The arrows point to an axon. Scale bar shown in the merged images is 10 μm.

island-P, which was completely unmethylated at every stage of development tested, was detected at either P1 or P14 (data not shown).

MeCP2 is involved in regulating expression of the novel *Shank3c* transcript

Next, we investigated the effect of MeCP2 on expression of the novel *Shank3c* transcripts. We prepared total RNA from neocortical tissue of *Mecp2*-deficient hemizygous male mice and wild-type littermates at the P7, P14, and P28 stages of development and performed a real-time RT-PCR. A previous electron-microscopic study revealed delayed neuronal development in *Mecp2*-deficient mice and that their nervous system contained numerous immature post-synaptic densities (Fukuda *et al.* 2005). First, we investigated expression of post-synaptic density-95 (PSD-95) (Fig. 9a). Although at P7 there were no significant differences in the level of PSD-95 expression between the *Mecp2*-deficient mice and wild-type mice, after P14 the level of PSD-95 expression in the *Mecp2*-deficient mice was significantly lower than in the wild-type mice, findings that were consistent with the results of a previous study that had indicated delayed neuronal development and abnormal synapses in *Mecp2*-deficient mice (wild-type mice: P14, 1.318 ± 0.020 (mean ± SEM) and P28, 1.152 ± 0.040; *Mecp2*-deficient mice: P7, 0.907 ± 0.030, P14, 1.017 ± 0.071, and P28, 0.856 ± 0.062). We then investigated the level of expression of two different *Shank3* transcripts in *Mecp2*-deficient mice: the *Shank3a* transcript, the major form of *Shank3* that is expressed from the 5′ end of the *Shank3* gene containing exon 1 (Fig. 9b), and the novel *Shank3c* transcript, whose transcriptional initiation site is located in intron 10 (Fig. 9c). During development, the level of *Shank3a* expression in the *Mecp2*-deficient mice was significantly lower than in the wild-type mice (wild-type mice: P14, 1.565 ± 0.030 and P28, 1.316 ± 0.020; *Mecp2*-deficient mice: P7, 0.896 ± 0.009, P14, 1.067 ± 0.011, and P28, 0.647 ± 0.005). In contrast, at P7 there was no significant difference between the levels of expression of the novel *Shank3c* transcript in intron 10 in the *Mecp2*-deficient mice and wild-type mice. However, at P14 expression of the novel *Shank3c* transcript in the *Mecp2*-deficient mice was clearly lower than in the wild-type mice (wild-type mice: P14, 0.824 ± 0.052 and P28, 1.654 ± 0.056; *Mecp2*-deficient mice: P7, 0.931 ± 0.049, P14, 0.547 ± 0.014, and P28, 1.480 ± 0.102). Interestingly, since at P28 the level of expression of the novel *Shank3* transcript in the *Mecp2*-deficient mice was not significantly different from its level of expression in the wild-type mice, the ratio of expression at

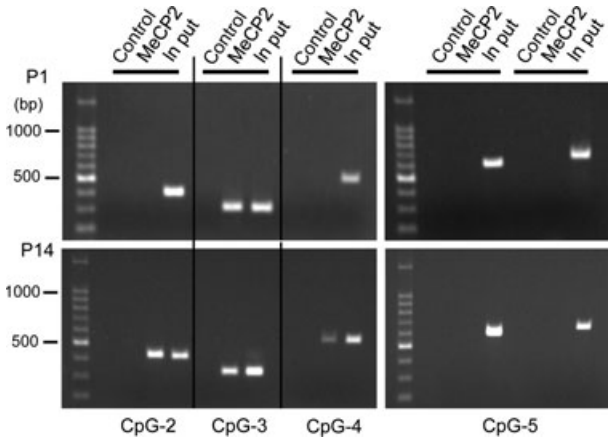

Fig. 8 Chromatin immunoprecipitation assay of mouse neocortex at P1 and P14. Representative agarose gel electrophoresis image showing binding of MeCP2 to CpG island-2, -3, -4, and -5. Normal rabbit IgG (control) and anti-MeCP2 antibody (MeCP2) were used to immunoprecipitate the genomic region of each CpG island. Size markers (100 bp ladder) are shown at the left.

P28 to expression at P14 in the *Mecp2*-deficient mice was significantly higher than in wild-type mice (wild-type mice: 2.02 ± 0.14 fold; *Mecp2*-deficient mice: 2.70 ± 0.21 fold, $p = 0.0098$, $n = 4$). These results suggested that MeCP2 is involved in regulating expression of the novel *Shank3c* transcript in intron 10.

Discussion

In this study, we identified two novel splicing *Shank3* transcript variants whose transcriptional initiation sites are located in intron 10. Sequence analysis revealed that the major *Shank3* transcript variant consisted of part of intron 10 and a completely spliced form from exon 11 to exon 22. We then demonstrated that the predicted translational start codon is located at position −77 in intron 10. Thus, this novel *Shank3* transcript probably produced the amino-terminus truncated SHANK3 isoform containing the Src homology 3 and following domains, including the post-synaptic density 95/discs large/zone occludens-1 domain, the homer-binding region, the cortactin-binding region, and SAM at its carboxyl-terminus. We investigated its expression profile in the developing mouse neocortex by performing a quantitative RT-PCR and immunoblot analysis. The transient decrease in its expression at P14 shown in Fig. 2 is unique. The result of the immunoblot analysis suggested that the lower expression of the transcript at P14 might be responsible for the reduction in protein after P14, especially at P21 (Fig. 6). Interestingly, the DNA methylation rate in CpG island-2, which is located near the transcriptional initiation site of the novel *Shank3* transcript and its promoter, increased at P14 and MeCP2 bound the CpG island-2 region. On the basis of the role of MeCP2 in transcriptional regulator via binding to the methylated DNA (Chahrour *et al.* 2008; Hite *et al.* 2009), we hypothesized that expression of the novel *Shank3* transcript is regulated by MeCP2. To test our hypothesis, we investigated expression of the novel *Shank3* transcript in *Mecp2*-deficient mice. Since a previous study showed that the synapses of *Mecp2*-deficient mice were less mature than in wild-type mice (Fukuda *et al.* 2005), we initially examined the expression of PSD-95 at P7, P14, and P28, and the results showed lower expression in *Mecp2*-deficient mice after P14, as expected. The level of expression of the full-length *Shank3* (*Shank3a*) transcript was also lower in *Mecp2*-deficient mice than in wild-type mice, especially at P14 and P28, when synapses were immature. We also demonstrated a difference between the expression profiles of the novel *Shank3* transcript (*Shank3c*) in wild-type mice and *Mecp2*-deficient mice. The rate of increase in expression level of the novel *Shank3* transcript from P14 to P28 was significantly higher than in the wild-type mice. These findings suggest that *Shank3* may be one of the target genes of MeCP2 and that the unbalanced expression of *Shank3* transcripts is implicated in the etiology of the synaptic abnormality caused by the dysfunction of MeCP2 in Rett syndrome.

Cumulative evidence has shown that several SHANK3 isoforms in human and rodent brains are produced as a result of complex transcriptional regulation by multiple intragenic promoters and extensive alternative splicing processes, and six different SHANK3 isoforms (SHANK3a-f) have been demonstrated thus far (Wang *et al.* 2011; Jiang and Ehlers 2013). Judging from gene and protein structures, the novel *Shank3* transcripts identified in this study likely code the SHANK3c isoforms reported in recent papers (Wang *et al.* 2011; Jiang and Ehlers 2013). Both papers reported demonstrating that the *Shank3c* transcript is expressed under promoter 3 located in intron 10, but the reports regarding the transcriptional initiation site of the *Shank3c* transcript are confusing. In Wang's paper, the transcriptional initiation site of the *Shank3*c transcript is reported to be located in intron 11, and two transcripts (*Shank3c-1* and *Shank3c-2*; GenBank: HQ405757 and HQ405758) are shown originating at the same initiation site. Since the transcriptional initiation site of *Shank3c-1* and *Shank3c-2* is different from that of the 22t *Shank3* transcript expressed in intron 11, they are not identical to the 22t *Shank3* transcript (Maunakea *et al.* 2010). On the other hand, the transcriptional initiation site reported in the review article by Jiang and Ehlers is located in intron 10. Based on all the above taken together, since the novel *Shank3* transcript identified in this study is one of the *Shank3c* transcripts, we designated it *Shank3c-3* (GenBank: AB841411). The other variant identified in the present study, designated *Shank3c-4* (GenBank: AB841412), lacks the sequences coded by exon 21, which results in production of the carboxyl-terminus truncated SHANK3 lacking the homer-binding region, the cortactin-binding region and the SAM. We identified a difference in the distribution of

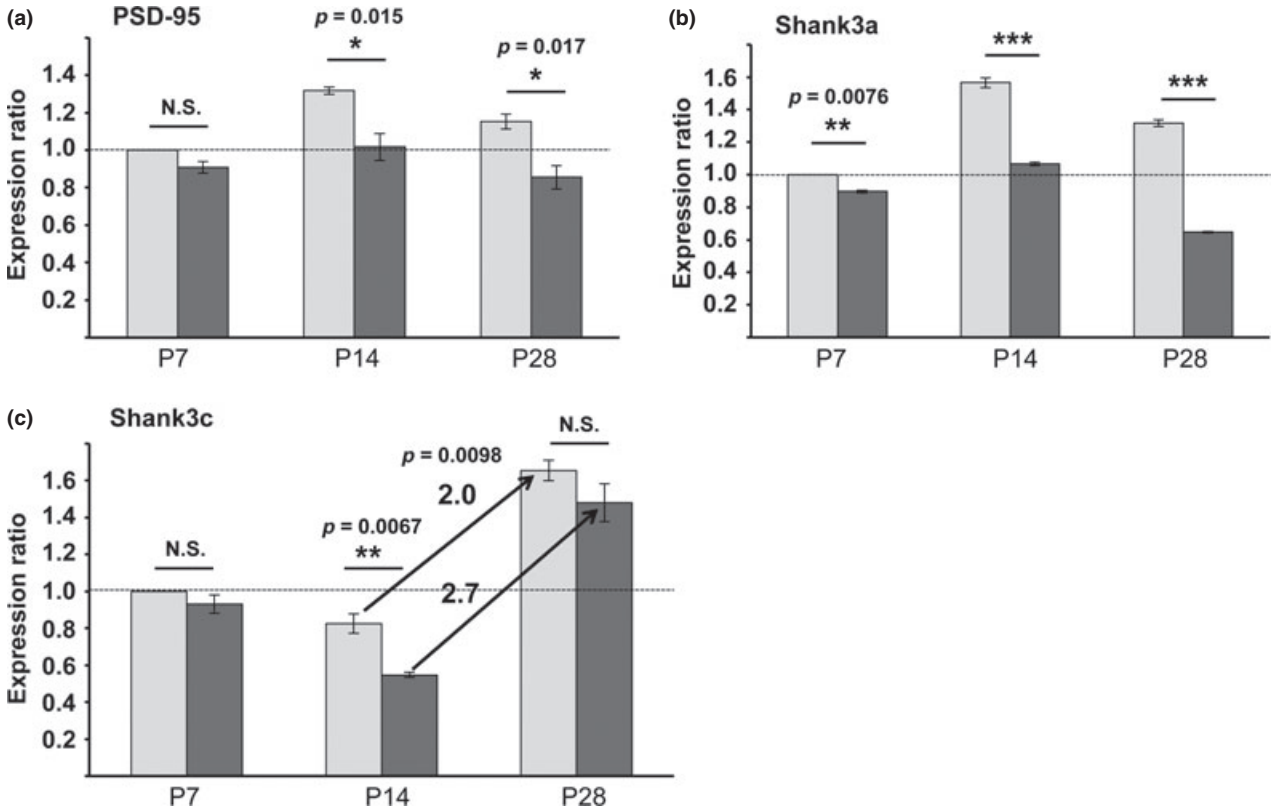

Fig. 9 Analysis of expression of the novel *Shank3* transcript in *Mecp2*-deficient mice by a real-time PCR. Neocortical samples were prepared at P7, P14, and P28, and real-time PCR was performed to investigate the expression of PSD-95 (a), the major form of *Shank3* amplified by the 5UTR-F and CpGP-R primer pair (Shank3a) (b), and the novel *Shank3* transcript amplified by the In10-F and Ex14-R primer pair (Shank3c) (c). A quantitative analysis was performed by the delta-delta Ct method with glyceraldehyde-3-phosphate dehydrogenase as an internal control. Ratios were calculated by dividing the value at each stage by the value at P7 in wild-type mice. Light gray columns represent the wild-type mice and dark gray columns represent the *Mecp2*-deficient mice. The real-time PCR was independently performed four times with triplet samples from each individual. More than three pups at each stage were obtained from more than two families. $*p < 0.05$, $**p < 0.01$, $***p < 0.001$, N.S. = not significant.

the isoform containing the entire carboxyl-terminus sequence in the primary cultured neurons and the distribution of the isoform lacking the sequences coded by exon 21. As shown in Figure 7, SHANK3c-3 was predominantly expressed in the dendritic spines, whereas SHANK3c-4 was diffusely expressed in both the dendrites and axons. These findings were highly consistent with the results of a previous study that showed that the carboxyl-terminus truncated SHANK3 lacking the cortactin-binding region and the SAM were not targeted to synapses and were diffusely distributed throughout the neurons (Boeckers *et al.* 2005). Interestingly, the *Shank3b* transcript (GenBank: AJ245904) is known to be one of the alternative splicing variants of *Shank3* (Jiang and Ehlers 2013). Since the predicted translational start site is located in intron 2, and the sequence coded by exon 21 is absent in the *Shank3b* transcript, the product of the *Shank3b* transcript contains ankyrin repeats but no homer-binding region, cortactin-binding region, and SAM, however, the expression profile of the *Shank3b* transcript has not been elucidated. On the other hand, a recent genetic study of ASD patients identified two siblings who were heterozygous for a guanine residue insertion in exon 21 that resulted in a frameshift and a carboxyl-terminus truncated SHANK3 protein lacking the homer-binding region and following regions (SHANK3ΔC) (Durand *et al.* 2007). Thus, the presence of the carboxyl-terminus truncated SHANK3 isoforms, including the *Shank3b* transcript and the splicing variant of the novel *Shank3* transcript expressed from intron 10 (*Shank3c-4*), may be essential in the brain, but regulation of their expression is critical to organize synaptic function, and abnormal expression of carboxyl-terminus truncated SHANK3 may cause brain dysfunction, including ASD.

Several lines of *Shank3* mutant mice have been generated recently. Targeting of exons 4–9 (Bozdagi *et al.* 2010; Wang *et al.* 2011; Yang *et al.* 2012) and exons 4–7 (Peça *et al.* 2011) resulted in the disruption of full-length SHANK3 (SHANK3a) and SHANK3b, but SHANK3c-f remained. The targeting of exons 13–16 (Peça *et al.* 2011), on the

other hand, led to the elimination of SHANK3c-d in addition to SHANK3a and SHANK3b. *Shank3* mutant mice exhibit a variety of behavioral deficits, including compulsive and repetitive behavior, enhanced anxiety, and impaired social interaction, all of which resemble the cardinal features of ASD. Furthermore, Schmeisser and coworkers produced a *Shank3* mutant mouse strain in which exon 11 was targeted (Schmeisser *et al.* 2012). Their *Shank3* mutant mouse can produce SHANK3d-f but not SHANK3a-c, but the results of a behavioral analysis have not yet been reported. As a means of identifying the brain region and neural cells that are related to the behavioral deficits caused by the disruption of SHANK3, we used the Cre/LoxP system to develop a conditional knockout mouse in which the genomic region from intron10 to intron 12 is targeted. The ability to spatiotemporally disrupt SHANK3a-c isoforms in a Cre-recombinase-expression-dependent manner makes it possible to investigate the function of the SHANK3 isoforms in individual brain regions. Our next study is designed to reveal the genetic and protein structures of SHANK3 isoforms and to clarify their contributions in the neuronal network that causes autistic behaviors.

Acknowledgements

This study was supported by grants from the Ministry of Health, Labour and Welfare of Japan (SU), the Ministry of Education, Culture, Sports, and Science and Technology of Japan (CW), and The Japan Foundation for Pediatric Research (SU). The authors have no conflicts of interest to declare.

Supporting information

Additional supporting information may be found in the online version of this article at the publisher's web-site:

Figure S1. Schematic diagram of the construction of EGFP expression vector pGL3-In10-EGFP by a two-step PCR method.

Figure S2. Schematic diagram of the construction of the myc-tagged SHANK3 isoform expression vectors, pCAGGS-myc-Shank3c-3 and pCAGGS-myc-Shank3c-4.

Data S1. Plasmid construction.

References

Amir R. E., Van den Veyver I. B., Wan M., Tran C. Q., Francke U. and Zoghbi H. Y. (1999) Rett syndrome is caused by mutations in X-linked *MECP2*, encoding methyl-CpG-binding protein 2. *Nat. Genet.* **23**, 185–188.

Beri S., Tonna N., Menozzi G., Bonaglia M. C., Sala C. and Giorda R. (2007) DNA methylation regulates tissue-specific expression of Shank3. *J. Neurochem.* **101**, 1380–1391.

Boeckers T. M., Segger-Junius M., Iglauer P., Bockmann J., Gundelfinger E. D., Kreutz M. R., Richter D., Kindler S. and Kreienkamp H.-J. (2004) Differential expression and dendritic transcript localization of Shank family members: identification of a dendritic targeting element in 3' untranslated region of Shank1 mRNA. *Mol. Cell. Neurosci.* **26**, 182–190.

Boeckers T. M., Liedtke T., Spilker C., Dresbach T., Bockmann J., Kreutz M. R. and Gundelfinger E. D. (2005) C-terminal synaptic targeting elements for postsynaptic density proteins ProSAP1/Shank2 and ProSAP2/Shank3. *J. Neurochem.* **92**, 519–524.

Bonaglia M. C., Giorda R., Borgatti R., Felisari G., Gagliardi C., Selicorni A. and Zuffardi O. (2001) Disruption of the ProSAP2 gene in a t(12;22)(q24.1;q13.3) is associated with the 22q13.3 deletion syndrome. *Am. J. Hum. Genet.* **69**, 261–268.

Bozdagi O., Sakurai T., Papapetrou D. *et al.* (2010) Haploinsufficiency of the autism-associated *Shank3* gene leads to deficits in synaptic function, social interaction, and social communication. *Mol. Autism* **1**, 15.

Chahrour M., Jung S. Y., Shaw C., Zhou X., Wong S. T. C., Qin J. and Zoghbi H. Y. (2008) MeCP2, a key contributor to neurological disease, activates and represses transcription. *Science* **320**, 1224–1229.

Ching T.-T., Maunakea A. K., Jun P. *et al.* (2005) Epigenome analyses using BAC microarrays identify evolutionary conservation of tissue-specific methylation of SHANK3. *Nat. Genet.* **37**, 645–651.

Chomczynski P. and Sacchi N. (1987) single-step method of RNA isolation by acid guanidinium thiocyanate-phenol-chloroform extraction. *Anal. Biochem.* **162**, 156–159.

Durand C. M., Betancur C., Boeckers T. M. *et al.* (2007) Mutations in the gene encoding the synaptic scaffolding protein SHANK3 are associated with autism spectrum disorders. *Nat. Genet.* **39**, 25–27.

Ermolinsky B., Pacheco Otalora L. F., Arshadmansab M. F., Zarei M. M. and Garrido-Sanabria E. R. (2008) Differential changes in mGlu2 and mGlu3 gene expression following pilocarpine-induced status epilepticus: a comparative real-time PCR analysis. *Brain Res.* **1226**, 173–180.

Fukuda T., Itoh M., Ichikawa T., Eashiyama K. and Goto Y. (2005) Delayed maturation of neuronal architecture and synaptogenesis in cerebral cortex of *Mecp2*-deficient mice. *J. Neuropathol. Exp. Neurol.* **64**, 537–544.

Gauthier J., Spiegelman D., Piton A. *et al.* (2009) Novel de novo SHANK3 mutation in autistic patients. *Am. J. Med. Genet. Part B.* **150B**, 421–424.

Guy J., Hendrich B., Holmes M., Martin J. E. and Bird A. (2001) A mouse Mecp2-null mutation causes neurological symptoms that mimic Rett syndrome. *Nat. Genet.* **27**, 322–326.

Hirasawa T., Wada H., Kohsaka S. and Uchino S. (2003) Inhibition of NMDA receptors induces delayed neuronal maturation and sustained proliferation of progenitor cells during neocortical development. *J. Neurosci. Res.* **74**, 676–687.

Hite K. C., Adams V. H. and Hansen J. C. (2009) Recent advances in MeCP2 structure and function. *Biochem. Cell Biol.* **87**, 219–227.

Jiang Y.-H. and Ehlers M. D. (2013) Modeling autism by *SHANK* gene mutations in mice. *Neuron* **78**, 8–27.

Lam C.-W. (2000) Spectrum of mutations in the *MECP2* gene in patients with infantile autism and Rett syndrome. *J. Med. Genet.* **37**, E14.

Lim S., Naisbitt S., Yoon J., Hwang J.-I., Suh P.-G., Sheng M. and Kim E. (1999) Characterization of the Shank family of synaptic proteins. Multiple genes, alternative splicing, and differential expression in brain and development. *J. Biol. Chem.* **274**, 29510–29518.

Maunakea A. K., Nagarajan R. P., Bilenky M. *et al.* (2010) Conserved role of intragenic DNA methylation in regulating alternative promoter. *Nature* **466**, 253–257.

Moessner R., Marshall C. R., Sutcliffe J. S. *et al.* (2007) Contribution of *SHANK3* mutations to autism spectrum disorder. *Am. J. Hum. Genet.* **81**, 1289–1297.

Naisbitt S., Kim E., Tu J. C., Xiao B., Sala C., Valtsvhanoff J., Weinberg R. J., Worley P. E. and Sheng M. (1999) Shank3, a novel family of postsynaptic density proteins that binds to the NMDA receptor/PSD-95/GKAP complex and cortactin. *Neuron* **23**, 569–582.

Peça J., Feliciano C., Ting J. T., Wang W., Wells M. F., Venkatraman T. N., Lascola C. D., Fu Z. and Feng G. (2011) *Shank3* mutant mice display autistic-like behaviours and striatal dysfunction. *Nature* **472**, 437–442.

Schmeisser M. J., Ey E., Wegener S. *et al.* (2012) Autistic-like behaviours and hyperactivity in mice lacking ProSAP1/Shank2. *Nature* **486**, 261–265.

Sheng M. and Kim E. (2000) The Shank family of scaffold proteins. *J. Cell Sci.* **113**, 1851–1856.

Uchino S., Wada H., Honda S., Nakamura Y., Ondo Y., Uchiyama T., Tsutsumi M., Suzuki E., Hirasawa T. and Kohsaka S. (2006) Direct interaction of post-synaptic density-95/Dlg/ZO-1 domain-containing synaptic molecule Shank3 with GluR1 α-amino-3-hydroxy-5-methyl-4-isoxazole propionic acid receptor. *J. Neurochem.* **97**, 1203–1214.

Waga C., Okamoto N., Ondo Y., Fukumura-Kato R., Goto Y., Kohsaka S. and Uchino S. (2011) Novel variants of the *SHANK3* gene in Japanese autistic patients with severe delayed speech development. *Psychiat. Genet.* **21**, 208–211.

Wang X., McCoy P. A., Rodriguiz R. M. *et al.* (2011) Synaptic dysfunction and abnormal behaviors in mice lacking major isoforms of *Shank3*. *Hum. Mol. Genet.* **20**, 3093–3108.

Yamada Y., Watanabe H., Miura F., Soejima H., Uchiyama M., Iwasaka T., Mukai T., Sakaki Y. and Ito T. (2004) A comprehensive analysis of allelic methylation status of CpG islands on human chromosome 21q. *Genome Res.* **14**, 247–266.

Yang M., Bozdagi O., Scattoni M. L. *et al.* (2012) Reduced excitatory neurotransmission and mild autism-relevant phenotypes in adolescent *Shank3* null mutant mice. *J. Neurosci.* **32**, 6525–6541.